ISBN: 978-3-95450-238-7 ISSN: 2226-0358 doi:10.18429/JACoW-ICALEPCS2023-M03A002

IMPLEMENTATION OF MODEL PREDICTIVE CONTROL FOR SLOW ORBIT FEEDBACK CONTROL IN MAX IV ACCELERATORS USING PyTango FRAMEWORK

Carla Takahashi*, Aureo Freitas, Magnus Sjöström, Jonas Breunlin
MAX IV Laboratory, Lund, Sweden
Emory Jensen Gassheld, My Karlsson, Pontus Giselsson, LTH, Lund, Sweden

Abstract

Achieving low emittance and high brightness in modern light sources requires stable beams, which are commonly achieved through feedback solutions. The MAX IV light source has two feedback systems, Fast Orbit Feedback (FOFB) and Slow Orbit Feedback (SOFB), operating in overlapping frequency regions. Currently in MAX IV, a general feedback device implemented in PyTango is used for slow orbit and trajectory correction, but an MPC controller for the beam orbit has been proposed to improve system robustness. The controller uses iterative optimisation of the system model, current measurements, dynamic states and system constraints to calculate changes in the controlled variables. The new device implements the MPC model according to the beam orbit response matrix, subscribes to change events on all beam position attributes and updates the control signal given to the slow magnets with a 10 Hz rate. This project aims to improve system robustness and reduce actuator saturation. The use of PyTango simplifies the implementation of the MPC controller by allowing access to high-level optimisation and control packages. This project will contribute to the development of a high-quality feedback control system for MAX IV accelerators.

INTRODUCTION

MAX IV Laboratory is a fourth-generation synchrotron light-source facility comprising a 3 GeV storage ring, a 1.5 GeV storage ring, and a linear accelerator, which serves a dual role as a full-energy injector into the storage rings and as the driving source for the Short Pulse Facility. Annually, the laboratory accommodates approximately 1000 users spanning academia, research institutes, industry, and government agencies, all of whom gain access to the facility through dedicated user access programs. Remarkably, MAX IV consistently delivers beam currents of 400 mA and 500 mA on the 3 GeV and 1.5 GeV storage rings, respectively, meeting the diverse experimental requirements of its user community.

The control system at MAX IV is structured in a three-layer architecture. At its core, the middle layer employs the TANGO[1] distributed control framework, effectively serving as the interface between the multitude of equipment within the facility and the oversight of their operations. Crucial tasks are managed by dedicated hardware components, ensuring reliable and precise operation. Above everything, from top client layer, users are able to employ Python and Matlab scripting languages to interface with the TANGO system.

Orbit Feedback on MAX IV

Transverse stability of the beam is an important aspect of achieving the low emittance and high brightness goals of any modern light source. This is commonly achieved via feedback solutions but the implementations vary; at the MAX IV light source there are two separate feedback systems working together in two different but overlapping frequency regions as well as sets of sensors. The Fast Orbit Feedback, so named because of its 10 kHz repetition rate, is capable of attenuating noise up to 50 – 150 Hz in the most critical regions. This is hardware-based controller based on Libera Brillance Plus beam position monitor systems. However, it also has the disadvantage of relying on relatively weak actuators that easily saturate. The SOFB controller, which on its own handles noise and orbit drifts from DC up to roughly 50 mHz, therefore also periodically off-loads the FOFB. It also covers the complete set of sensors. In contrast to the FOFB the SOFB, working at much lower rates, could be and was implemented in software as a feedback device in TANGO [2, 3].

The sensors of the both the FOFB and the SOFB systems are Beam Position Monitors (BPMs), for the horizontal and vertical planes, which are read out using commercial Libera Brilliance Plus electronics. Overall, there are 200 BPMs in the 3 GeV ring for each of the horizontal and vertical planes and 36 BPMs per plane on the 1.5 GeV ring. These devices are interfaced in TANGO and the beam positions in both planes are available as attributes. The attributes push events at the 10 Hz rate of the slow Libera data acquisition stream, which provides 2 Hz BW position data. The events are are timestamped according to the local clock in the Libera crate, which is synced via NTP, so the position data from all BPMs are read and pushed every 0.1 s stamped with the same hardware time [4].

The actuators in the SOFB are the slow corrector magnets controlled by ITest BILT BE2811 power supplies. There are 380 power supplies in the 3 GeV ring, in which 200 drive horizontal plan magnets and 180 are used in the vertical plane, and 72 in the 1.5 GeV ring, 36 in each plane. Previous timing studies were performed to confirm that these can handle remote commands to change the current output at 10 Hz. However the power supplies of the corrector magnets often saturate, which sometimes require human intervention

* carla.takahashi@maxiv.lu.se

Content from this work may be used under the terms of the CC BY 4.0 licence (© 2023). Any distribution of this work must maintain attribution to the author(s), title of the work, publisher, and DOI

ISBN: 978-3-95450-238-7 ISSN: 2226-0358 doi:10.18429/JACoW-ICALEPCS2023-M03A002

to drive the system into a working condition. Thus, an alternative control strategy became necessary to improve the orbit correction system's robustness and reliability.

Model Predictive Control

Model Predictive Control is type of controller that, as indicated by its name, predicts the expected response of the dependent variables of the modeled system to changes on the independent variables. Overall, MPC uses an iterative optimization of the model system to compute a control signal by minimizing the control cost for a given horizon time [5, 6]. At each iteration point, the MPC uses the current measurements of the plant variables, dynamic states of the system (such as the ones given by Kalman Filters), MPC models and the constraints of the system to calculate changes of the dependent variables in the given horizon. With this, the controller attempts to keep the dependent variables on target, while respecting all system constraints. In general, at each iteration, the MPC should apply only the first change predicted for the independent variables and reevaluate all predictions on the next iteration.

One of the most significant advantages of MPC is that the controller explicitly handles constraints which can be physical limits or safety limits on states and control signals [7]. Fundamentally, MPC also borrows many characteristics of optimal control which provides robustness against modelling imprecision and nominal stability under specific constraints. Due to the same underlying reason, MPC also inherently handles multi-input multi-output (MIMO) plants and time delays. Furthermore, known disturbances can be incorporated into the MPC to improve the controller response [6].

CONTROL SYSTEMS BACKGROUND

Model Predictive Control Design

Similarly to optimal control methods, the implementation of an MPC requires a model of plant to be controlled. This can be a linear discrete model, which can be described by a state space representation such as in Eq. (1) [5, 7]:

$$\begin{aligned} x_{k+1} &= \Phi x_k + \Gamma u_k \\ y_k &= C x_k \end{aligned} \tag{1}$$

in which $x_k \in \mathbb{R}^n$ are the states at time k, $u_k \in \mathbb{R}^m$ are the control signals at time k, $y_k \in \mathbb{R}^l$ are the outputs at time k, and $\Phi \in \mathbb{R}^{m\times m}$, $\Gamma \in \mathbb{R}^{m\times n}$ and $C \in \mathbb{R}^{l\times m}$ are the model state, input and output matrices.

Model Predictive Control uses models to explicitly predict future plant behaviour. For this purpose, the MPC, at time k, solves an open loop optimal control problem over a predefined finite horizon and apply the first control signal. Afterwards, for the time $k+1$, it repeats the same procedure using previous optimal solution as initial guess. Essentially, the estimation of any given state can be determined by Eq. (2) and, analogously, the prediction of a state over a finite horizon H_p is obtained according to Eq. (3):

$$x_k = \Phi^k x_0 + \sum_{j=0}^{k-1} \Phi^j \Gamma u_{k-1-j} \tag{2}$$

$$x_{k+H_p} = \Phi^{H_p} x_k + \sum_{i=0}^{H_p-1} \Phi^j \Gamma u_{k+H_p-1-j} \tag{3}$$

Thus, the predicted system output is given by:

$$y_k = C\left(\Phi^k x_0 + \sum_{j=0}^{k-1} \Phi^j \Gamma u_{k-1-j}\right) \tag{4}$$

$$y_{k+H_p} = C\left(\Phi^{H_p} x_k + \sum_{i=0}^{H_p-1} \Phi^j \Gamma u_{k+H_p-1-j}\right) \tag{5}$$

Considering that the primary objectives of a control feedback system are the minimization of the tracking error and control cost, MPCs solve minimization constrained problems in which the objective cost function aggregates the estimation error and the control changes [5, 7], as shown in Eq. (6):

$$J = \sum_{i=k+1}^{k+H_p-1} e_i^T Q_1 e_i + \sum_{i=k}^{k+H_u-1} \Delta u_i^T Q_2 \Delta u_i + e_{k+H_p}^T Q_f e_{k+H_p} \tag{6}$$

in which, the error is defined in Eq. (7), and the control signal change is defined in Eq. (8).

$$e_k = y_k - y_{ref} \tag{7}$$

$$\Delta u_k = u_k - u_{k-1} \tag{8}$$

The parameters H_p and H_u are the prediction and control horizons, respectively, and the matrices Q_1, Q_2 and Q_f are the state error, control signal and terminal state penalty functions. Therefore, it is possible to state that the first term penalizes tracking error, the second term penalizes control signal changes and the third therm penalizes the terminal state error. Finally, the optimization problem can be written

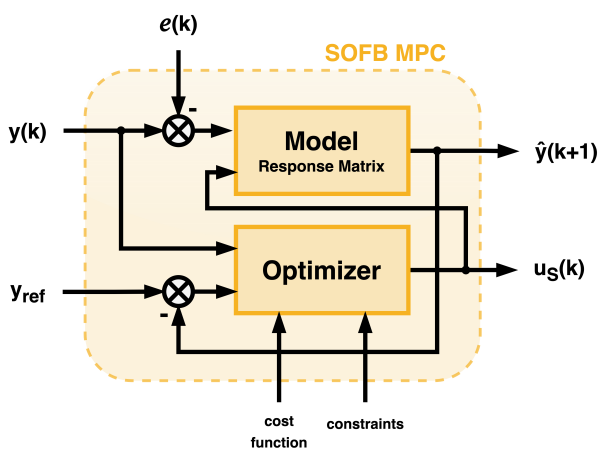

Figure 1: MPC bock diagram.

Content from this work may be used under the terms of the CC BY 4.0 licence (© 2023). Any distribution of this work must maintain attribution to the author(s), title of the work, publisher, and DOI

ISBN: 978-3-95450-238-7 ISSN: 2226-0358 doi:10.18429/JACoW-ICALEPCS2023-MO3A002

Content from this work may be used under the terms of the CC BY 4.0 licence (© 2023). Any distribution of this work must maintain attribution to the author(s), title of the work, publisher, and DOI

according to Eq. (9) and the MPC controller can be illustrated with the diagram in Fig. 1 [5, 7].

$$\begin{aligned} \min_{x,u} \quad & J = \sum_{i=k+1}^{k+H_p-1} e_i^T Q_1 e_i + \sum_{i=k}^{k+H_u-1} \Delta u_i^T Q_2 \Delta u_i \\ & + e_{k+H_p}^T Q_f e_{k+H_p} \\ \text{s.t.} \quad & x_{k+1} = \Phi x_k + \Gamma u_k \\ & y_k = C x_k \\ & \bar{x} = x_0 \\ & |x| \leq x_{\max} \\ & |u| \leq u_{\max} \end{aligned} \tag{9}$$

Mid-Range Control

Often, the control of real-world plants can become very complex due to their structure, restrictions and requirements, thus bottom-up strategies allow high-level control systems to be designed with interconnected standard control loops. In this context, the architecture of the control system will vary according to the available sensors, actuators and observable states. When multiple sensors are available for a single control signal, a Cascade control strategy can be implemented. Analogously, the dual problem where multiple actuators are available to control a single measured target allows the development of a mid-range control architecture [8].

SLOW ORBIT FEEDBACK MODEL PREDICTIVE CONTROL DEVELOPMENT

Controller Design

Orbit Model In the context of the Slow Orbit Feedback control, the beam orbit is monitored by the BPMs, which will be considered our sensors or output values, and the corrector magnets are the actuators, therefore the control signal is the current applied by the power supplies that drive them. Thus, the system model should reflect the relation between the BPMs and the corrector magnets currents. This relationship is commonly referred as Response Matrix (R). At MAX IV, the response matrix is highly linear on the operational range and the Horizontal and vertical plane a almost completely decoupled. This allows the control system to be divided into two complete separated subsystems per storage ring. Essentially, the plant can be well described by Eq. (10) [3]:

$$y_k = P_y(z)\, R P_u(z)\, u_k + d_k \tag{10}$$

where $P_y(z)$ and $P_u(z)$ are diagonal matrices containing the sensor and actuator dynamics, respectively, and d represent orbits disturbances. The ring model (10) can be rewritten according (1) as:

$$\begin{aligned} x_{k+1} &= \Phi x_k + R P_u(z)\, \Delta u_k \\ y_k &= P_y(z)\, x_k \end{aligned} \tag{11}$$

in which Φ, $P_y(z)$ and $P_u(z)$ are considered, at the moment, identity matrices. Thus, the constraints of the optimization model in Eq. (9) can be defined according to plant physical constraints. The actuators power supplies saturation limits are symmetrical around zero and are used to define $u_{\max}$. The maximum allowed position deviation around the reference can be used to define $x_{\max}$.

RF Adjustment At the same time, the corrector magnets cause a energy shift along the longitudinal plane of the beam, which described by the orbit lengthening model [7, 9]. This change in energy comprises a linear and a quadratic component, where the quadratic component is negligible compared to the linear component, thus allowing the it to be described by Eq. (12):

$$\frac{\Delta E}{E} = -\frac{1}{L_0 \alpha} \eta_A^T u \tag{12}$$

where η_A is given by the dispersion function, L_0 is the circumference of the storage ring and α is the momentum compaction factor. This beam distortion can be compensated by adjusting the orbit frequency according to Eq. (13):

$$\frac{\Delta E}{E} = -\frac{1}{\alpha} \frac{\Delta f}{f} \tag{13}$$

where

$$\Delta f_k = f_k - f_{k-1} \tag{14}$$

However, the change of the radio frequency also affects the position of the beam according to Eq. (15):

$$\Delta y = -\frac{1}{\alpha} \eta_S^T \Delta f \tag{15}$$

where η_S is given by the dispersion function of the BPMs and describes how much a change in the frequency affects the sensor readings. Thus, the plant model can be extended to include the Rf compensation terms resulting the the following Eq. (16) [7]:

$$\begin{aligned} \begin{bmatrix} x \\ x_f \end{bmatrix}_{k+1} &= I \begin{bmatrix} x \\ x_f \end{bmatrix}_k + \begin{bmatrix} R & -\frac{1}{\alpha}\eta_S \\ -\frac{1}{L_0 \alpha}\eta_A^T & -\frac{1}{\alpha f} \end{bmatrix} \begin{bmatrix} \Delta u \\ \Delta f \end{bmatrix}_k \\ \begin{bmatrix} y \\ \frac{\Delta E}{E} \end{bmatrix}_k &= I \begin{bmatrix} x \\ x_f \end{bmatrix}_k \end{aligned} \tag{16}$$

FOFB Offloading The integration with the Fast Orbit Feedback Control is done during two different stages. First, at every iteration of the slow orbit feedback, the fast orbit expected sensor values are updated to match the next values estimated by the MPC, one step ahead. However, the fast correctors rely on relatively weak actuators that easily saturate. To mitigate this issue the slow orbit feedback system adjusts the operational point of the FOFB back into the middle of the operation range, in a process named here FOFB offloading that happends every 5 s. For that purpose, the average error of the BPMs computed by the fast orbit control loop is subtracted from the sensor reference, which forces the slow orbit control loop to apply a stronger correction compensation towards the point where the FOFB is actually

ISBN: 978-3-95450-238-7 ISSN: 2226-0358 doi:10.18429/JACoW-ICALEPCS2023-M03A002

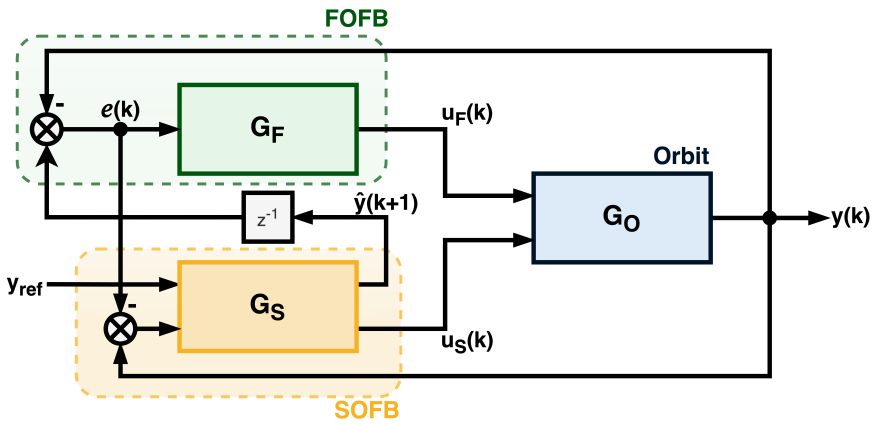

Figure 2: Orbit feedback control system diagram.

operating. With this, the corrections that were done by the FOFB are overtaken by the SOFB, reducing the load on the FOFB.

In a comprehensive sense, the Orbit feedback system can be implemented as a mid-range control architecture where the SOFB and FOFB loops are interconnected, as represented in Fig. 2.

Tango Device Implementation

The SOFB MPC controller was implemented in the distributed system layer using PyTango [10] framework, which is the Python module that exposes to Python the complete Tango C++ API. This allowed the employment of the dompc [11] open-source toolbox for robust model predictive control.

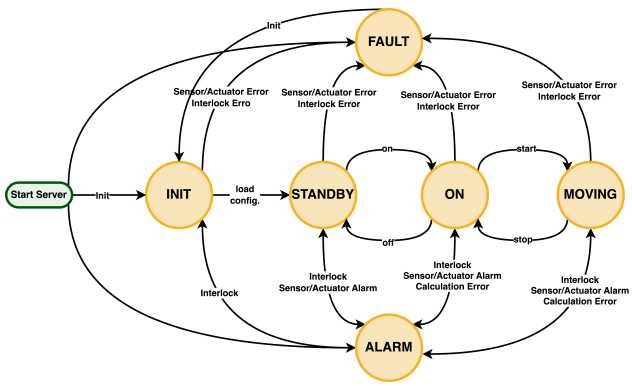

Figure 3: State machine pf the SOFB MPC Tango Device.

The state machine of the the SOFB MPC controller, in Fig. 3, allows the controller to transition between STANDBY, ON and MOVING states through user triggered commands. When the controller is on STANDBY, it is completely configured but is not performing any calculations or adjusting the control signal. The ON state implies that the controller is calculating the control signal for the current input signals but the correction is not being applied. When MOVING, the controller is calculating the correction and applying the changes on the control signal. Whenever a transition to the MOVING state occurs, the MPC data history is cleared to prevent outdated estimations, therefore the initial values of the states are updated with the current sensor values [12]. The ALARM and FAULT states indicates that the device is not operating properly. While the ALARM state indicates a transient issue which allows the device to return to operation after the problems are resolved, the FAULT state, however, indicates are more sever issue which requires re initialization and reconfiguration of the Tango device.

The sensor readout is event based, in this context, the device has a dedicated thread in which the event listeners captures change events sent by the Libera BPM devices on the position attributes. The thread proceeds to aggregate the all the events received according to the timestamp of each event [12], as illustrated in Fig. 4. In this context, the sensor values are considered valid when events were received from all BPMs within a tolerance time frame.

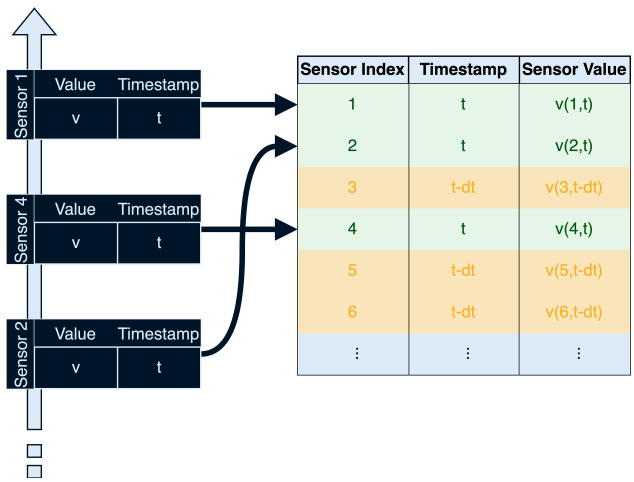

Figure 4: Sensors events handling.

Content from this work may be used under the terms of the CC BY 4.0 licence (© 2023). Any distribution of this work must maintain attribution to the author(s), title of the work, publisher, and DOI

ISBN: 978-3-95450-238-7 ISSN: 2226-0358 doi:10.18429/JACoW-ICALEPCS2023-M03A002

CONTROLLER APPLICATION AT MAX IV

SOFB MPC Device Setup

The configuration and initialization with the device can be done through Tango's standard GUIs, Jive and Atk Panel, additionally the PyTango Client API in Python or its Matlab binding can be used to interact with the Device. The Interlock, RF adjustment and FOFB device name configurations are done through properties stored on the Tango Database, therefore they can be defined in Jive. All other parameters of the controller and model, including sensor and actuators devices names are stored in device attributes and need to configured whenever the device is started, with the aid of the ATK Panel or by using a script in python or Matlab.

Control Loop Response

The MPC controller Tango Device was tested on storage rings of MAX IV during non user delivery weeks. Within this particular circumstance, the beam orbit could, mainly, be subjected to anticipated disturbances.

(a) Sensor values

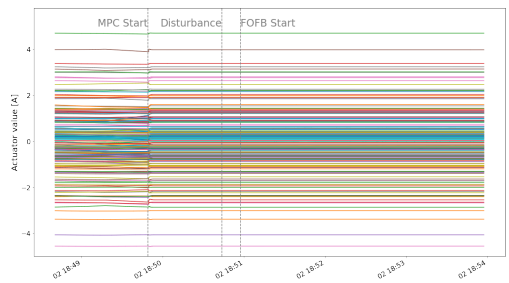

(b) Actuator values

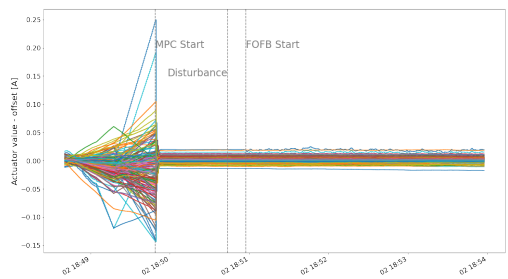

(c) Actuator Values minus offset

Figure 5: MPC tests on the 3 GeV ring horizontal plane with initial states distant from set point.

During the tests on the storage rings horizontal planes, it was noticed that the initial overshoot is significant and, ideally, this should be reduced. For instance, on the 3 GeV ring the overshoot is around 200 µm, as shown in Fig. 5a, which is a significant deviation of the beam position which leaves little margin to the safety limits of the plant and approaches a beam dump condition. Furthermore, the amplitude of the overshoot significantly depends on the initial conditions of the plant, as observed in Fig. 6a, if the initial states are closer to the optimal ones, the overshoot is significantly smaller, around 2 µm. However, this also indicates that the initial overshoot might actually cause a beam dump if the initial states are sufficiently far from the optimal ones.

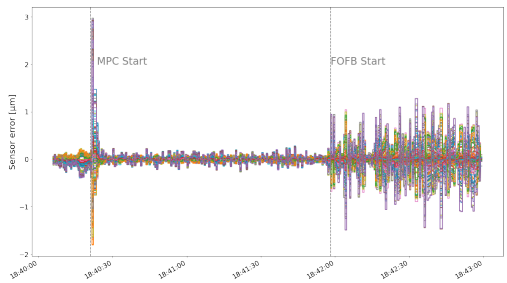

(a) Sensor values

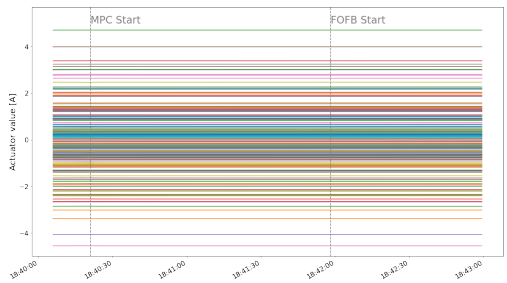

(b) Actuator values

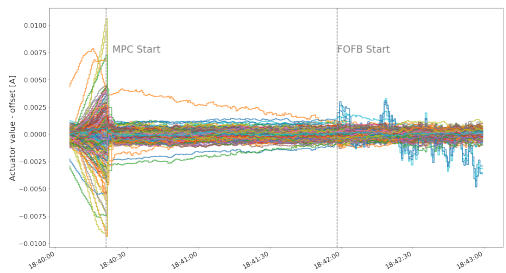

(c) Actuator Values minus offset

Figure 6: MPC tests on the 3 GeV ring horizontal plane with initial states near set point.

It was possible to simulate slow disturbances by ramping down the fast correctors to zero while the FOFB system was off. On Figs. 5 and 7, it is possible to see that the the MPC responded to the disturbance with small variation on the control signal and minimal disturbance on the sensor readings. Since the FOFB system works at a much higher frequency and rely on faster sensors, it will react to some noise that is filtered on the SOFB, Therefore the fast orbit control loop introduces some noise into the system when it is turned on during a steady state operation without any disturbances as observed ion the tests in Figs. 5, 6 and 7.

Content from this work may be used under the terms of the CC BY 4.0 licence (© 2023). Any distribution of this work must maintain attribution to the author(s), title of the work, publisher, and DOI

ISBN: 978-3-95450-238-7 ISSN: 2226-0358 doi:10.18429/JACoW-ICALEPCS2023-M03A002

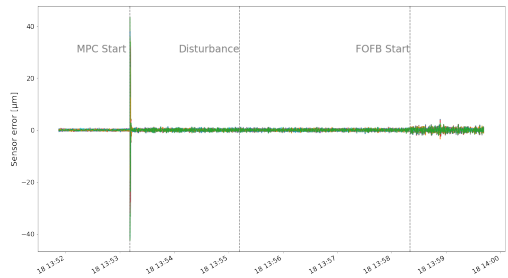

(a) Sensor values

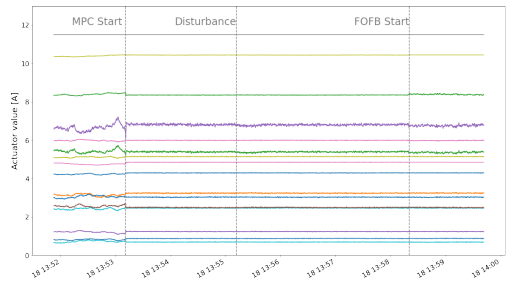

(b) Actuator values

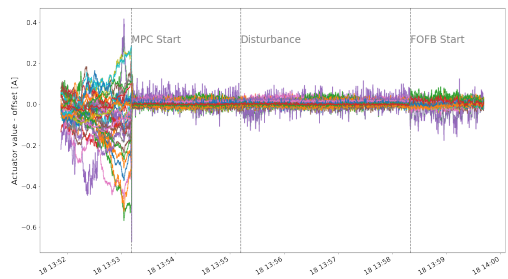

(c) Actuator Values minus offset

Figure 7: MPC tests on the 1.5 GeV ring horizontal plane.

During steady state operation, the MPC controller presented good performance and low levels of noise, when external disturbances were not present. Some of the actuators started working nearer the saturation limits but did not saturate. During tests, it was possible to noticed that the MPC was capable of recovering the orbit from disturbances that shifted the beam to positions where the traditional controller could not operate without saturating the actuators. Furthermore, the MPC was able to recover the orbit when some actuators were saturated. Since Δu was one of the MPC optimization model parameters, the control signal variation should be limited on steady state operation. This can be observed on Figs. 5c, 6c and 7c, where the mean, or offset, of the each control signal was subtracted from it.

FUTURE DEVELOPMENTS

There are clear possible improvements to the MPC device. Initially it is possible to extend the model to incorporate transient characteristics of the sensors and actuators, this would increase the prediction horizon and improve the controller response, specially on higher operational rates. Furthermore it is possible to improve the initial estimation of the system by incorporating the current value of the actuators as well. Additionally, uncertainty and disturbance models can be added to the controller in order to improve prediction with longer horizons.

CONCLUSION

The MPC controller achieves good error levels on steady-state operation and has a fast response on transitions. The overshoot in transitions, specially on the start of the control action, can be mitigated with more strict constraints on the state values, furthermore, the incorporation of the current actuator values on the initial estimation may also improve this. As expected, the MPC causes the controller to work closer to the saturation point of the actuators without reaching it. Additionally, the controller is capable of recovering from undesired states without saturating the actuators.

ACKNOWLEDGEMENTS

The authors would like to thank the Software group and the physicists, engineers and operators of the accelerators, without the collaboration of whom this work would not have been possible. Also, the authors would like to thank MAX IV, the Technical Division and the Accelerator Division for their support.

REFERENCES

[1] Tango controls, http://www.tango-controls.org

[2] P. F. Tavares *et al.*, "Commissioning and first-year operational results of the MAXIV 3GeV ring", *J. Synchrotron Radiat.*, vol. 25, no. 5, pp. 1291–1316, 2018. doi:10.1107/S1600577518008111

[3] M. Sjöström, J. Ahlback, M. A. G. Johansson, S. C. Leemann, and R. Nilsson, "Orbit Feedback System for the MAX IV 3 GeV Storage Ring", in *Proc. IPAC'11*, San Sebastian, Spain, 2011, pp. 499–501. https://jacow.org/IPAC2011/papers/MOPO010.pdf

[4] A. Freitas, V. Hardion, M. Lindberg, R. Lindvall, R. Sv?ñrd, and C. Takahashi, "Control System Suite for Beam Position Monitors at MAX IV", in *Proc. IBIC'22*, Kraków, Poland, 2022, pp. 496–499. doi:10.18429/JACoW-IBIC2022-WEP38

[5] J. B. Rawlings, D. Q. Mayne, and M. M. Diehl, *Model Predictive Control: Theory, Computation, and Design*, 2nd. Nob Hill Publishing, LLC, 2022.

[6] What is model predictive control?, https://se.mathworks.com/help/mpc/gs/what-is-mpc.html

[7] E. Gassheld and M. Karlsson, "MPC for the slow orbit feedback control at MAX IV", submitted for publication.

[8] K. Åström and T. Hägglund, *Advanced PID Control*, English. ISA - The Instrumentation, Systems and Automation Society, 2006.

[9] J. Wenninger, "Orbit corrector magnets and beam energy", CERN, Rep. SL-Note-97-06-OP, 1997.

[10] Pytango, https://pytango.readthedocs.io

Content from this work may be used under the terms of the CC BY 4.0 licence (© 2023). Any distribution of this work must maintain attribution to the author(s), title of the work, publisher, and DOI

ISBN: 978-3-95450-238-7 ISSN: 2226-0358 doi:10.18429/JACoW-ICALEPCS2023-M03A002

[11] F. Fiedler *et al.*, "Do-mpc: Towards FAIR nonlinear and robust model predictive control", *Control Engineering Practice*, vol. 140, p. 105 676, 2023. doi:10.1016/j.conengprac.2023.105676

[12] P. J. Bell, V. H. Hardion, M. Lindberg, V. Martos, and M. Sjöström, "A general multiple-input multiple-output feedback device in Tango for the MAX IV accelerators", in *Proc. ICALEPCS'19*, New York, NY, USA, 2020, p. 1085. doi:10.18429/JACoW-ICALEPCS2019-WEPHA012

Content from this work may be used under the terms of the CC BY 4.0 licence (© 2023). Any distribution of this work must maintain attribution to the author(s), title of the work, publisher, and DOI